

Stable explicit depth extrapolation of seismic wavefields

Dave Hale*

ABSTRACT

Stability has traditionally been one of the most compelling advantages of implicit methods for seismic wavefield extrapolation. The common 45-degree, finite-difference migration algorithm, for example, is based on an implicit wavefield extrapolation that is guaranteed to be stable. Specifically, wavefield energy will not grow exponentially with depth as the wavefield is extrapolated downwards into the subsurface. Explicit methods, in contrast, tend to be unstable. Without special care in their implementation, explicit extrapolation methods cause wavefield energy to grow exponentially with depth, contrary to physical expectations.

The Taylor series method may be used to design finite-length, explicit, extrapolation filters. In the usual Taylor series method, N coefficients of a finite-length filter are chosen to match N terms in a truncated

Taylor series approximation of the desired filter's Fourier transform. Unfortunately, this method yields unstable extrapolation filters. However, a simple modification of the Taylor series method yields extrapolators that are stable.

The accuracy of stable explicit extrapolators is determined by their length—longer extrapolators yield accurate extrapolation for a wider range of propagation angles than do shorter filters. Because a very long extrapolator is required to extrapolate waves propagating at angles approaching 90 degrees, stable explicit extrapolators *may* be less efficient than implicit extrapolators for high propagation angles. For more modest propagation angles of 50 degrees or less, stable explicit extrapolators are likely to be more efficient than current implicit extrapolators. Furthermore, unlike implicit extrapolators, stable explicit extrapolators naturally attenuate waves propagating at high angles for which the extrapolators are inaccurate.

INTRODUCTION

Implicit filtering methods are widely used to extrapolate seismic wavefields in depth. For example, the well-known 45-degree, finite-difference method for depth migration is based on a recursive application of implicit filtering (e.g., Claerbout, 1985). Implicit methods are most attractive because they are guaranteed to be stable. Specifically, implicit methods for depth extrapolation will not permit the amplitude of the extrapolated wavefield to grow with depth. In contrast, the most straightforward explicit extrapolation methods are unstable, tending to amplify wavefield amplitudes exponentially with depth.

Notwithstanding stability, explicit filtering is attractive because it resembles convolution, for which each filtered output sample can be computed independently, perhaps in parallel with other output samples. Implicit filtering, in contrast, is accomplished by solving a linear system of

coupled equations for the filtered output samples. Partly because it is simpler, explicit filtering is likely to be implemented more efficiently on various computer architectures (vector, parallel, super-scalar, etc.) than is implicit filtering.

In addition to simplicity, another advantage of explicit methods for depth extrapolation of seismic wavefields is the ease with which explicit methods can be extended for use in 3-D depth migration. The solution of the linear system of equations required by implicit methods is particularly awkward in this application. For example, an accurate extension of the implicit 45-degree, finite-difference method to 3-D depth migration is difficult and may be computationally impractical (Claerbout, 1985, p. 101; Yilmaz, 1987, p. 405). Explicit depth extrapolation methods, in contrast, are easily extended to 3-D depth migration, as demonstrated by Blacquièrre et al. (1989).

These advantages of computational simplicity, efficiency, and extendability motivate the development of a method for

Manuscript received by the Editor August 16, 1990; revised manuscript received February 20, 1991.

*Department of Geophysics, Colorado School of Mines, Golden, CO 80401.

© 1991 Society of Exploration Geophysicists. All rights reserved.

designing *stable* explicit depth extrapolation filters. In addition to discussing these advantages, Holberg (1988) describes a constrained least-squares method for designing explicit extrapolation filters. Unfortunately, as illustrated below, repeated application of filters designed by a least-squares method may lead to instability and/or exponential decay with depth for certain frequencies (and wavenumbers) in the seismic wavefield.

In the spirit of Holberg's work, this paper addresses the following filter design problem:

Find N coefficients h_n of a finite-length filter with a Fourier transform $H(k)$ that approximates the desired Fourier transform of an extrapolation filter defined by

$$D(k) \equiv \exp \left\{ i \left(\frac{\Delta z}{\Delta x} \right) \left[\left(\frac{\omega \Delta x}{v} \right)^2 - k^2 \right]^{1/2} \right\}, \quad (1)$$

for $|k| \leq |\omega \Delta x / v|$, subject to the constraint that $|H(k)| \leq 1$ for $|k| \leq \pi$.

In this definition of $D(k)$, ω denotes frequency (in radians per unit time), v denotes velocity, and Δz and Δx denote vertical and horizontal spatial sampling intervals, respectively. Wavenumber k (measured in radians per sample in the x direction) is normalized such that any distance quantity is measured in terms of the number of horizontal sampling intervals Δx . With this normalization, two dimensionless constants, $\Delta z / \Delta x$ and $\omega \Delta x / v$, uniquely determine the desired transform $D(k)$.

The desired transform $D(k)$ defined by equation (1) is the filter one might apply in the phase-shift method of migration developed by Gazdag (1978), in situations where velocity v varies only with depth z . However, explicit extrapolators can easily handle lateral velocity variations. As suggested by Holberg (1988), one first computes a table of extrapolators for a typical range of normalized frequencies, $\omega \Delta x / v$. Then, in extrapolating from one depth to the next, lateral velocity variations are handled by letting the filter coefficients h_n vary laterally as the value of normalized frequency changes with velocity. In other words, lateral velocity variations are handled by a laterally varying extrapolator.

The desired filter is appropriate for waves traveling one way, either down or up. In depth extrapolation of common mid-point (CMP) stacked data, which corresponds to waves propagating both down and up, we may use the "exploding reflectors" concept and replace velocity v with half-velocity $v/2$ (e.g., Claerbout, 1985). This replacement is implied by references to half-velocity below.

The symmetry of the desired transform $D(k)$ with respect to k implies that the complex extrapolation filter coefficients h_n should be even. Specifically, we expect $h_{-n} = h_n$. Therefore, the number of coefficients N should be odd, with the coefficient index n bounded by $-(N - 1)/2 \leq n \leq (N - 1)/2$.

EXPLICIT EXTRAPOLATORS FOR A SINGLE FREQUENCY

Figure 1 illustrates amplitude spectra $|H(k)|$ for three explicit, 19-coefficient extrapolators, as a function of normalized wavenumber (measured in cycles). In this example, $\Delta z = \Delta x$ and normalized frequency $\omega \Delta x / v = \pi/2$ radians.

Therefore, the right half of this figure corresponds to evanescent waves for which $|k| > |\omega \Delta x / v|$.

The curve labeled "Least-Squares" corresponds to an extrapolator designed by an *unconstrained* least-squares method that is equivalent to simply inverse Fourier transforming the desired transform $D(k)$ and truncating to the desired number of coefficients $N = 19$. In this example, the desired $D(k)$ was assumed to be $D(\omega \Delta x / v) = 1$ for $|k| > |\omega \Delta x / v|$. Other choices for this evanescent region yielded greater errors than those exhibited in Figure 1. The amplitude spectrum of this extrapolator has a ripply character that is typical of filters designed by least-squares methods. Note that the amplitude is greater than one for some wavenumbers; Fourier components of a seismic wavefield corresponding to these wavenumbers will grow exponentially as this extrapolator is applied repeatedly in the recursive process of depth extrapolation. Likewise, amplitudes less than one correspond to exponential decay of the corresponding wavenumbers.

The curve labeled "Taylor Series" in Figure 1 corresponds to an extrapolator that was designed by a conventional Taylor series method, in which the $N = 19$ coefficients were chosen to match the first nineteen terms in a Taylor series expansion of the desired transform. Specifically, the first nineteen terms of the Taylor series expansion about $k = 0$ were determined for both the desired Fourier transform $D(k)$ and the actual Fourier transform $H(k)$. Because $H(k)$ is a linear function of the unknown filter coefficients h_n , equating the first nineteen terms of the Taylor series yields a system of nineteen linear equations that may be solved for the coefficients h_n . The symmetry $h_{-n} = h_n$ was exploited to reduce the number of linear equations from $N = 19$ to $(N + 1)/2 = 10$. As the amplitude spectrum of Figure 1 indicates, the extrapolator obtained with this method is quite unstable, particularly for the evanescent wavenumbers.

The curve labeled "Modified Taylor Series" in Figure 1 corresponds to a 19-coefficient extrapolator that was designed by a modified Taylor series method, which is de-

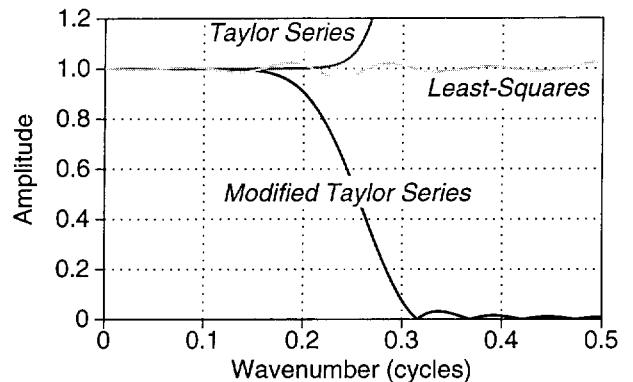


FIG. 1. Amplitude spectra for 19-coefficient explicit extrapolators designed by an unconstrained least-squares method (light gray), the conventional Taylor series method (dark gray), and the modified Taylor series method described in Appendix A (black). In this figure (and in Figures 2-4), normalized wavenumbers greater than 0.25 correspond to evanescent waves.

scribed in detail in Appendix A. In this method, the $N = 19$ coefficients were determined by matching only the first eleven terms in the Taylor series expansions of the desired and actual Fourier transforms. The remaining $N - 11 = 8$ degrees of freedom were used to force the amplitude spectrum to zero at uniformly-spaced wavenumbers in the evanescent region. Because the amplitude spectrum in Figure 1 is never greater than one, this extrapolator is stable for all wavenumbers. Note that this extrapolator attenuates high wavenumbers, with most of the attenuation occurring in the evanescent region.

Figure 2 is a detailed plot of the amplitude errors for the three extrapolators. As noted above, the ripply character of the least-squares (light gray) extrapolator is typical. Holberg (1988) has demonstrated that the magnitude of these oscillations can be significantly reduced by (1) restricting the range of wavenumbers for which the least-squares fit is attempted and (2) constraining the filter to be stable (amplitudes less than one) for wavenumbers outside this range. These constraints yield extrapolators with the same ripply character but with less amplitude error than that shown here for an unconstrained least-squares extrapolator.

Whereas amplitude errors in Figure 2 indicate stability (or instability), the phase errors plotted in Figures 3 and 4 indicate how well (or how poorly) explicit extrapolators will position reflectors in depth migration. The phase errors plotted in Figures 3 and 4 correspond to extrapolators with 19 and 39 coefficients, respectively. As expected, increasing the length of an extrapolator reduces its phase error.

Figures 3 and 4 suggest that a high price has been paid for stability. The stable extrapolator exhibits significantly greater phase error than either of the two unstable extrapolators.

EXPLICIT EXTRAPOLATORS FOR A RANGE OF FREQUENCIES

Figures 1 through 4 illustrate amplitude and phase errors of extrapolators designed for the particular normalized frequency $\omega\Delta x/v = \pi/2$ radians. In practice, extrapolation filters must be designed for a wide range of frequencies.

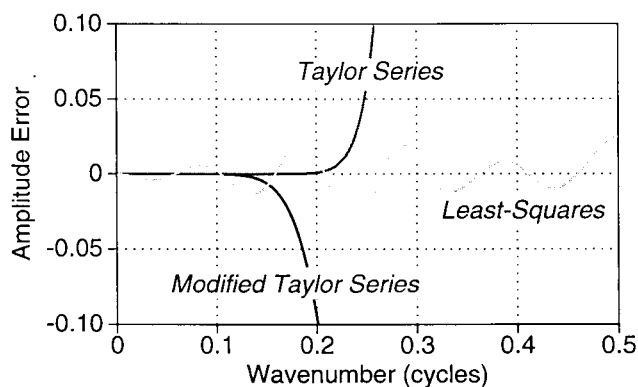


FIG. 2. Amplitude errors for 19-coefficient explicit extrapolators designed by an unconstrained least-squares method (light gray), the conventional Taylor series method (dark gray), and the modified Taylor series method described in Appendix A (black).

Figures 5 and 6 show contours of constant amplitude and phase error, respectively, for stable explicit extrapolators with 39 coefficients designed by the modified Taylor series method described above. Errors are plotted as a function of normalized frequency and wave propagation angle.

As in the preceding examples, $\Delta z = \Delta x$ was used in designing these stable extrapolators. For each normalized frequency, a system of linear equations was solved to match terms in the Taylor series expansions of the desired and actual Fourier transforms. In the modified Taylor series method, fewer than $N = 39$ terms are matched to obtain a stable extrapolator; the number of terms that can be matched while maintaining stability increases with the value of normalized frequency. The jagged nature of the contours in Figures 5 and 6 is caused by changes in this number of terms matched, which must be an integer.

For convenience in using these figures, the normalized frequency axis has been labeled in cycles (instead of radians), ranging from 0.0 to 0.5 cycles. For example, the combination of a frequency of 40 Hz, a CMP spacing of 12.5

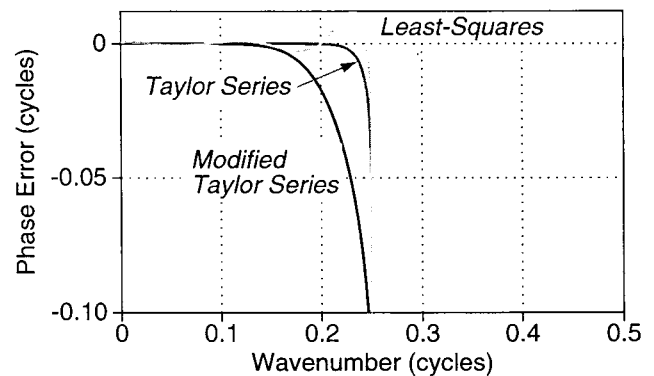


FIG. 3. Phase errors for 19-coefficient explicit extrapolators designed by an unconstrained least-squares method (light gray), the conventional Taylor series method (dark gray), and the modified Taylor series method described in Appendix A (black).

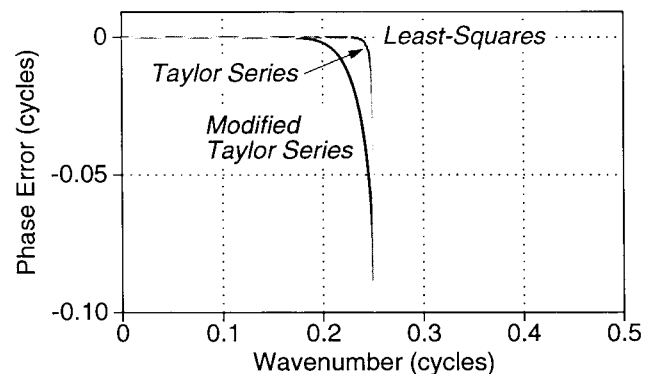


FIG. 4. Phase errors for 39-coefficient explicit extrapolators designed by an unconstrained least-squares method (light gray), the conventional Taylor series method (dark gray), and the modified Taylor series method described in Appendix A (black). Compare with Figure 3.

m, and a velocity (or half-velocity) of 1 km/s corresponds to a normalized frequency of 0.5 cycles. Normalized frequency can easily be computed for other choices of these parameters, and the computed values will typically fall inside the range 0.0 to 0.5 cycles.

Amplitude error for stable extrapolators is contoured in Figure 5 for errors of $-1/1000$, $-1/100$, and $-1/10$, corresponding to thin, medium, and thick contours, respectively. (Thick contours imply large errors). Figure 5 shows that, in one extrapolation step, stable extrapolators will attenuate waves propagating at an angle of 50 degrees by a factor of 0.999 for most frequencies. After 1000 such extrapolation steps, these waves will have been attenuated by a factor of 0.999 raised to the 1000th power, which is approximately $1/e \approx 0.37$.

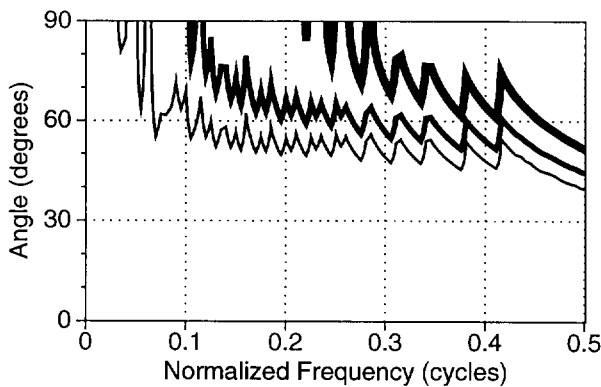


FIG. 5. Amplitude error contours for a 39-coefficient explicit extrapolator designed by the modified Taylor series method described in Appendix A. Error is contoured as a function of normalized frequency and propagation angle (measured from vertical). Normalized (dimensionless) frequency is frequency (Hz) times the horizontal sampling interval (km) divided by velocity (km/s). Contour values are $-1/1000$ (thin), $-1/100$ (medium), and $-1/10$ (thick).

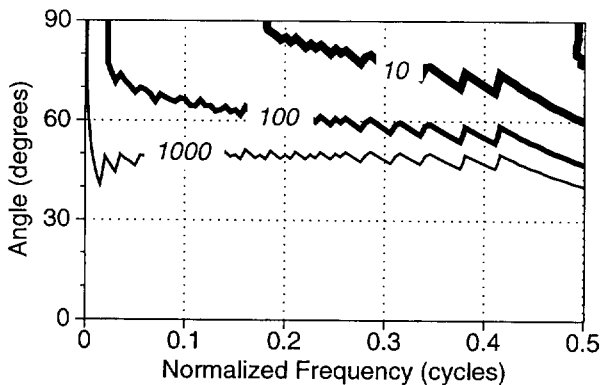


FIG. 6. Phase error contours for a 39-coefficient explicit extrapolator designed by the modified Taylor series method described in Appendix A. Error is contoured as a function of normalized frequency and propagation angle (measured from vertical). Normalized (dimensionless) frequency is frequency (Hz) times the horizontal sampling interval (km) divided by velocity (km/s). Contours are labeled with the number of extrapolation steps required to accumulate one-half cycle of phase error.

Phase error for stable extrapolators is contoured in Figure 6 for errors of $-\pi/1000$, $-\pi/100$, and $-\pi/10$, corresponding to thin, medium, and thick contours, respectively. (Again, thick contours imply large errors.) Since phase errors accumulate, Figure 6 shows, for example, that these stable explicit extrapolators yield one-half cycle (π radians) of phase error after 1000 extrapolation steps for waves propagating at an angle of about 50 degrees. Therefore, each of the contours in Figure 6 is annotated with the number of steps required to accumulate one-half cycle of phase error.

Comparison of Figures 5 and 6 suggests that waves propagating at very high angles will be attenuated, so that only those propagation angles for which the stable extrapolators are accurate will be preserved during depth extrapolation. In other words, a depth migration process based on these extrapolators will attenuate steeply dipping reflectors that would otherwise be mispositioned due to large phase errors.

As suggested by Figures 3 and 4, the errors in stable explicit extrapolators may be reduced by using longer extrapolators. Likewise, shorter extrapolators yield greater errors. Although not shown here, a stable explicit extrapolator with 19 (instead of 39) coefficients yields one-half cycle of phase error after 1000 extrapolation steps for waves propagating at an angle of about 35 degrees. Therefore, about 15 degrees of propagation angle may be gained by approximately doubling the number of extrapolator coefficients from 19 to 39.

Note that the phase error in Figure 6 is more or less independent of frequency. In contrast, the phase error for implicit depth extrapolation is highly frequency-dependent. For comparison, phase error for a so-called "65-degree" implicit extrapolation filter (Lee and Suh, 1985) is contoured in Figure 7. The term "65-degree" refers to the accuracy in approximating the square-root in equation (1). Specifically, the 65-degree approximation is obtained by a slight adjustment of the coefficients of the more traditional 45-degree approximation to the square-root. The terms "45-degree"

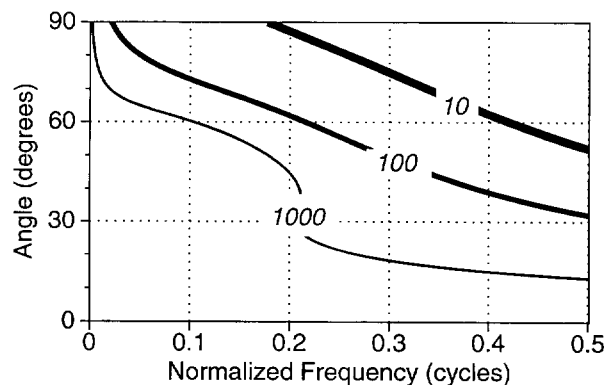


FIG. 7. Phase error contours for a so-called "65-degree" implicit extrapolator. Compare with Figure 6. Error is contoured as a function of normalized frequency and propagation angle (measured from vertical). Normalized (dimensionless) frequency is frequency (Hz) times the horizontal sampling interval (km) divided by velocity (km/s). Contours are labeled with the number of extrapolation steps required to accumulate one-half cycle of phase error.

and "65-degree" fail to account for errors in approximating spatial derivatives with finite differences; these are the errors that account for the increase in phase error with increasing normalized frequency evident in Figure 7.

Recalling the definition of normalized frequency above, the only parameter that may be adjusted in practice to reduce this phase error is the horizontal spatial sampling interval Δx . For the previous example of a frequency of 40 Hz and a half-velocity of 1 km/s, Figure 7 implies that $\Delta x = 1.25$ m would be required to obtain less than one-half cycle of phase error after 1000 extrapolation steps for a wave propagating at 65 degrees. This spatial sampling interval is a factor of 10 smaller than the 12.5 m necessary to avoid spatial aliasing. Given that $\Delta z = \Delta x$ for the extrapolators shown here, the size of each vertical depth step must be reduced accordingly, which implies that more steps are necessary to extrapolate to a particular depth. In practice, the high computational cost associated with such fine spatial sampling intervals suggests that 65-degree accuracy is rarely achieved with 65-degree implicit methods for depth migration.

For those wishing to reproduce the errors contoured in Figure 7, horizontal spatial derivatives were approximated here using the so-called "1/6 thick" described by Claerbout (1985, p. 262). A value of 1/12 was used here because it yields less phase error than the value 1/6 for the 65-degree approximation.

Implicit extrapolators, in principle, are capable of high accuracy for very high propagation angles. Figure 8 shows contours of phase error for a 90-degree implicit extrapolator. This extrapolator is obtained through a partial fraction expansion of the square-root in equation (1), as suggested by Ma (1981) and developed by Lee and Suh (1985). The computational cost of this extrapolator is approximately five times that of the 65-degree extrapolator. Again, note the frequency dependence of the phase error contours in Figure 8, which implies that small spatial sampling intervals are required to obtain 90-degree accuracy.

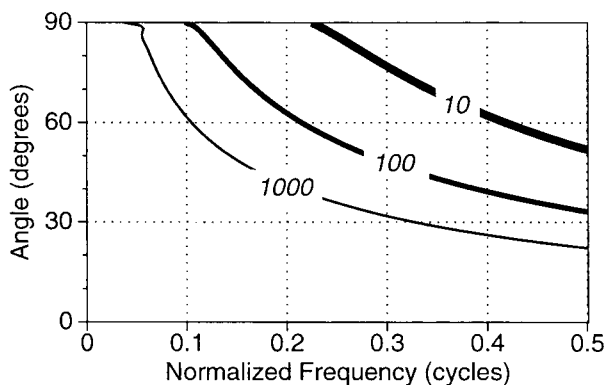


FIG. 8. Phase error contours for a so-called "90-degree" implicit extrapolator. Compare with Figures 6 and 7. Error is contoured as a function of normalized frequency and propagation angle (measured from vertical). Normalized (dimensionless) frequency is frequency (Hz) times the horizontal sampling interval (km) divided by velocity (km/s). Contours are labeled with the number of extrapolation steps required to accumulate one-half cycle of phase error.

MIGRATION IMPULSE RESPONSES

To further test the stable explicit extrapolators described above (and in Appendix A), a migration program was developed based on those extrapolators. Figure 9 exhibits migration impulse responses for a 19-coefficient stable explicit extrapolator. The input to the migration was a section containing just three nonzero samples. In this example, spatial sampling intervals $\Delta z = \Delta x = 10$ m, time sampling interval $\Delta t = 10$ ms, and half-velocity = 1 km/s. The maximum (Nyquist) frequency is 50 Hz = $1/(2\Delta t)$. Therefore, these data contain normalized frequencies ranging from 0.0 to 0.5, the same range represented in Figures 5 through 8. These parameters are representative of those one might encounter in processing recorded seismic data.

Note that steep dips (high propagation angles) are attenuated in Figure 9. Those dips that are present are correctly positioned along concentric semicircles with centers at the origin. No visible dispersion of low and high frequencies is exhibited by these impulse responses. Figure 10 illustrates the benefit of increasing the number of coefficients in stable explicit extrapolators from 19 to 39. Increasing the number of coefficients by roughly a factor of 2 has increased the dip limit of stable explicit extrapolators by about 15 degrees. Again, note that no visible dispersion of low and high frequencies is exhibited by these impulse responses. As indicated in Figure 6, and confirmed in Figure 10, the phase accuracy of stable explicit extrapolators is more or less independent of frequency.

For comparison, a 65-degree implicit migration yields the impulse responses shown in Figure 11. Note that the accuracy of this implicit method is frequency dependent. High frequencies are mis-positioned at steep dips, as suggested by the phase errors contoured in Figure 7. Also, note the heart-shaped character of the impulse responses. The particularly strong cusp at the center of each heart is dispersed evanescent energy contained in the impulses input to the migration. (See Claerbout, 1985, p. 247). Unlike the stable explicit extrapolation filters described here, implicit extrapolation filters do not naturally attenuate this evanescent energy.

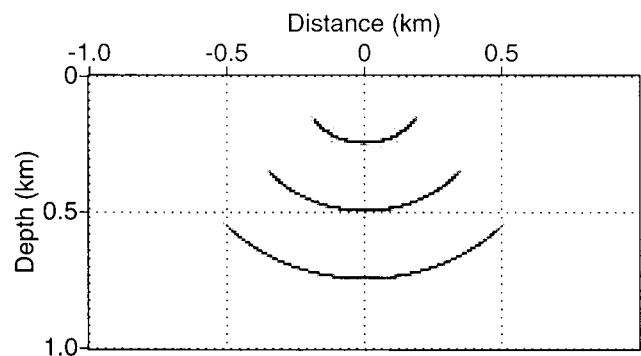


FIG. 9. Impulse responses of migration via 19-coefficient stable explicit extrapolators. Steep dips are attenuated, but dips remaining are correctly positioned along concentric semicircles with centers at the origin, with no visible dispersion of low and high frequencies.

CONCLUSIONS

Stable explicit filters for depth extrapolation of seismic wavefields may be derived through a modification of the conventional Taylor series method. The modified Taylor series method described here yields extrapolators with maximally-flat amplitude spectra in their passband, while ensuring that no spectral components in the wavefield are amplified by a factor greater than one.

The price for stability is increased phase error. The stable explicit extrapolators described here exhibit more phase error than do unstable extrapolators. Phase error in stable

(or unstable) explicit extrapolators may be reduced by increasing the number of coefficients in the extrapolation filter.

For low normalized frequencies, implicit extrapolators (Figures 7 and 8) are more accurate than the 39-coefficient stable extrapolator (Figure 6) described here. However, the small spatial sampling intervals required to obtain high phase accuracy in implicit extrapolation imply that this accuracy is rarely achieved in practice. Over the wide range of normalized frequencies likely to be encountered in practice, stable explicit extrapolators outperform implicit ones, except perhaps for propagation angles near 90 degrees.

The method presented here for deriving stable explicit extrapolators is in no formal sense optimal. It merely yields stable extrapolators. In my experience with alternative methods for designing stable extrapolators, the method presented here produced the least phase error while ensuring stability. Nevertheless, a simple method for designing optimal (in some sense) stable explicit extrapolators would be preferred over the method presented here.

ACKNOWLEDGMENTS

Thanks to Ken Lerner, Paul Fowler, Sam Gray, David Thompson, and an anonymous reviewer—their suggestions improved this paper significantly. Financial support for this work was provided in part by the United States Department of Energy, Grant Number DE-FG02-89ER14079. (This support does not constitute an endorsement by DOE of the views expressed in this paper.) Support was also provided by the members of the Consortium Project on Seismic Inverse Methods for Complex Structures at the Center for Wave Phenomena, Colorado School of Mines.

REFERENCES

- Blacquière, G., Debye, H. W. J., Wapenaar, C. P. A., and Berkhout, A. J., 1989, 3D table-driven migration: *Geophys. Prosp.*, **37**, 925–958.
- Claerbout, J. F., 1985, *Imaging the earth's interior*: Blackwell Scientific Publications, Inc.
- Gazdag, J., 1978, Wave equation migration with the phase-shift method: *Geophysics*, **43**, 1342–1351.
- Holberg, O., 1988, Towards optimum one-way wave propagation: *Geophys. Prosp.*, **36**, 99–114.
- Kaiser, J. F., 1979, Design subroutine (MXFLAT) for symmetric FIR lowpass digital filters with maximally-flat pass and stop bands, *in* Digital Signal Processing Committee of the IEEE ASSP Soc., Programs for Digital Signal Processing: IEEE Press, 5.3-1–5.3-6.
- Lee, M. W., and Suh, S. Y., 1985, Optimization of one-way wave equations: *Geophysics*, **50**, 1634–1637.
- Ma, Z., 1981, Finite-difference migration with higher-order approximation: Presented at the 1981 joint meeting of the China Geophys. Soc. and Soc. of Expl. Geophys., Beijing, China.
- Yilmaz, O., 1987, *Seismic Data Processing*: Soc. of Expl. Geophysics.

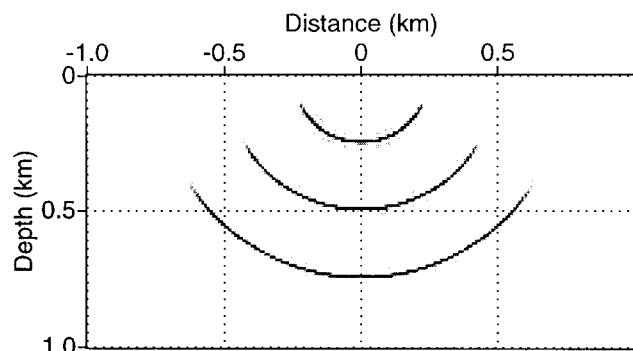


FIG. 10. Impulse responses of migration via 39-coefficient stable explicit extrapolators. Comparison with Figure 9 indicates that longer extrapolators yield steeper dips. As for Figure 9, note that the impulse responses are correctly positioned along concentric semicircles with centers at the origin, with no visible dispersion of low and high frequencies.

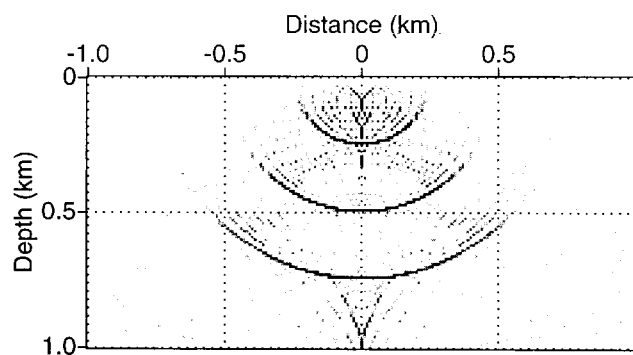


FIG. 11. Impulse responses of migration via 65-degree implicit extrapolators. Note the dispersion of low and high frequencies at steep dips. The heart-like shape of these impulse responses is dispersed evanescent energy not attenuated by implicit extrapolation. Compare with Figures 9 and 10.

APPENDIX A

DERIVATION OF STABLE EXTRAPOLATORS

Let h_n denote the N complex coefficients of a finite-length extrapolation filter. Because the extrapolation filter is symmetric (both the real and imaginary parts are even), N should be an odd number. The coefficient index n is bounded by $-(N - 1)/2 \leq n \leq (N - 1)/2$, and the filter is completely specified by only $(N + 1)/2$ complex coefficients. Define the Fourier transform of the extrapolation filter by

$$H(k) \equiv \sum_{n = -(N - 1)/2}^{(N - 1)/2} h_n e^{-ikn}.$$

Because h_n is symmetric,

$$H(k) = \sum_{n = 0}^{(N - 1)/2} (2 - \delta_{n0}) h_n \cos(kn),$$

where δ_{n0} is the Kronecker delta function defined by

$$\delta_{n0} \equiv \begin{cases} 1, & \text{if } n = 0; \\ 0, & \text{otherwise.} \end{cases}$$

In the conventional Taylor series method of designing the extrapolation filter h_n , the $(N + 1)/2$ distinct complex coefficients would be determined by equating derivatives of $H(k)$, the actual transform, with those of $D(k)$, the desired transform defined by equation (1) of the text. In particular, because the extrapolation filter is symmetric and we want this filter to be exact for waves propagating vertically, we would match the first $(N + 1)/2$ even derivatives at $k = 0$. As illustrated in Figure 1, this most straightforward application of the Taylor series method yields an unstable extrapolation filter, a filter for which $|H(k)| > 1$ for some wavenumbers k .

To obtain a stable filter, we must attempt to match fewer than $(N + 1)/2$ derivatives and let the remaining degrees of freedom in the filter be exploited to ensure $|H(k)| \leq 1$. In this modified Taylor series method, let the coefficients of the filter be represented as a sum of M weighted basis functions:

$$h_n = \sum_{m = 0}^{M - 1} c_m b_{mn}, \tag{A-1}$$

where, for reasons given below, a good choice for the basis functions is

$$b_{mn} = (2 - \delta_{m0}) \cos\left(\frac{2\pi mn}{N}\right). \tag{A-2}$$

Instead of determining $(N + 1)/2$ complex filter coefficients h_n , we will determine M complex weights c_m . For stability, the number, M , of weights must be less than the number, $(N + 1)/2$, of filter coefficients. Therefore, we will match only the first M even derivatives of the desired and actual Fourier transforms, using the remaining $(N + 1)/2 - M$ degrees of freedom to ensure stability.

In terms of the weights c_m to be determined, the Fourier transform of the extrapolation filter is

$$H(k) = \sum_{m = 0}^{M - 1} c_m (2 - \delta_{m0}) \sum_{n = 0}^{(N - 1)/2} (2 - \delta_{n0}) \times \cos\left(\frac{2\pi mn}{N}\right) \cos(kn) \tag{A-3}$$

$$= \sum_{m = 0}^{M - 1} c_m B_m(k), \tag{A-4}$$

where

$$B_m(k) \equiv (2 - \delta_{m0}) \sum_{n = 0}^{(N - 1)/2} (2 - \delta_{n0}) \times \cos\left(\frac{2\pi mn}{N}\right) \cos(kn) \tag{A-5}$$

are the Fourier transformed basis functions. Matching the ℓ th even derivative at $k = 0$, we obtain the linear equation

$$\sum_{m = 0}^{M - 1} c_m B_m^{(2\ell)}(0) = D^{(2\ell)}(0), \tag{A-6}$$

where

$$B_m^{(2\ell)}(0) = (2 - \delta_{m0}) (-1)^\ell \sum_{n = 0}^{(N - 1)/2} (2 - \delta_{n0}) \times \cos\left(\frac{2\pi mn}{N}\right) n^{2\ell}.$$

By matching M such even derivatives, for $\ell = 0, 1, \dots, M - 1$, we obtain a system of M linear equations for the unknown weights c_m . After solving this linear system for the weights c_m , we may use equations (A-1) and (A-2) to compute the extrapolation filter coefficients h_n .

In practice, the derivatives $D^{2\ell}(0)$ in the Taylor series expansion of the desired transform $D(k)$ [equation (1)] are best obtained with the help of a computer. For large ℓ , expressions for these derivatives become unwieldy, but they can be expressed in terms of the constants $\Delta z/\Delta x$ and $\omega \Delta x/v$, and a table of numerical coefficients. In computing the extrapolation filters illustrated in this paper, a computer program to perform symbolic differentiation was used to generate and store in a file the table of coefficients representing the first 40 terms of the Taylor series of the desired transform $D(k)$. This file (about 9000 bytes) was then directly included during compilation of the computer program (written in the C programming language) that computed the extrapolation filter coefficients.

The stability of the extrapolation filters derived via this modified Taylor series method lies in the definition of the basis functions b_{mn} in equation (A-2). Each of these basis functions, corresponding to $m = 0, 1, \dots, M - 1$, represents a particular range of wavenumbers k , with $m = 0$

representing the wavenumbers centered at $k = 0$. To see this, we analytically compute the Fourier transform of each basis function, according to equation (A-5). The Fourier transform of the m 'th basis function is

$$B_m(k) = \left(1 - \frac{\delta_{m0}}{2}\right) \left\{ \frac{\sin \left[\frac{N}{2} \left(k + \frac{2\pi m}{N} \right) \right]}{\sin \left[\frac{1}{2} \left(k + \frac{2\pi m}{N} \right) \right]} + \frac{\sin \left[\frac{N}{2} \left(k - \frac{2\pi m}{N} \right) \right]}{\sin \left[\frac{1}{2} \left(k - \frac{2\pi m}{N} \right) \right]} \right\}. \quad (\text{A-7})$$

These Fourier transformed basis functions are plotted in Figure A-1, for $M = 6$ and $N = 19$. For large N , each of the transforms in equation (A-7) is approximately equal to the sum of two sinc functions.

In the example illustrated in Figure A-1, four of the $(N + 1)/2 = 10$ degrees of freedom in the extrapolation filter are used to place four zeros in its Fourier transform for high wavenumbers k . Recall equation (A-4), which states that the Fourier transform of the extrapolation filter $H(k)$ is just a weighted sum of the Fourier transforms of the basis functions $B_m(k)$. Therefore, regardless of the weights c_m computed by matching derivatives in the modified Taylor series method, the Fourier transform of the extrapolation filter will

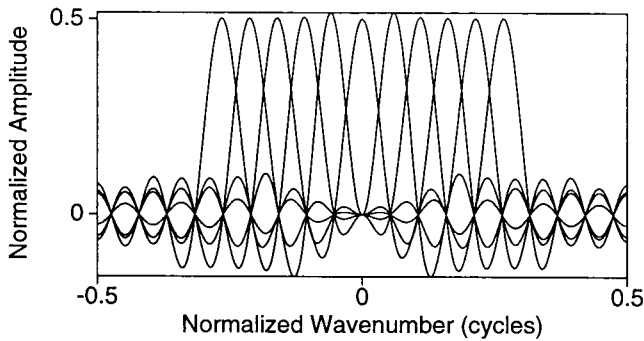


FIG. A-1. Fourier transforms of basis functions for $M = 6$ and $N = 19$. Note that, in this example, there are $(N + 1)/2 - M = 4$ uniformly spaced zeros at the high wavenumbers. These zeros attenuate evanescent waves and ensure stability of the corresponding extrapolation filter. The Fourier transform of the extrapolation filter is just a weighted sum of these sinc-like functions.

be forced to zero at four high wavenumbers k . It is at these higher wavenumbers that extrapolation filters derived via the conventional Taylor series method are most unstable. In this example, forcing the transform to zero at four high wavenumbers makes the extrapolation filter stable for all wavenumbers.

Unfortunately, the author knows of no analytical method for determining the number of zeros necessary to ensure stability for a given filter length N and constants $\Delta z/\Delta x$ and $\omega\Delta x/v$. The numerical method used here was to simply test different M , starting with $M = (N - 1)/2$ and decreasing M until a stable extrapolation filter was found. A conjecture of this paper, based only on the author's experience, is that useful, stable extrapolators can be found for some $M \leq (N - 1)/2$.

A stable, although not necessarily useful, extrapolator is guaranteed to exist. For $M = 1$, only the value (zeroth derivative) of the desired transform $D(k)$ is matched at $k = 0$. Although the extrapolator obtained for $M = 1$ may yield unacceptable phase error, it is guaranteed to be stable. From equations (A-1), (A-6), and (A-7), it is straightforward to show that, for $M = 1$, h_n has a Fourier transform $H(k)$ that satisfies the required constraint $|H(k)| \leq 1$. However, such an extrapolator exhibits acceptable phase error only for wave propagation angles near zero.

As illustrated in Figure 1 of the text, stable extrapolators derived using this modified Taylor series method tend to have their zeros at high wavenumbers corresponding to evanescent waves, inhomogeneous waves for which $|k| > |\omega\Delta x/v|$. The zeros attenuate evanescent waves and waves propagating at angles for which the extrapolation filter has significant error in phase, as illustrated by Figures 5 and 6.

The modification to the conventional Taylor series method described here is just one among many possible modifications. One likely alternative method that was tested is to solve $(N + 1)/2$ equations directly for the unknown filter coefficients h_n (without basis functions), with M of the equations used to match the first M even derivatives of $D(k)$ at $k = 0$ and the remaining $(N + 1)/2 - M$ equations used to zero the first $(N + 1)/2 - M$ even derivatives of the actual transform $H(k)$ at $k = \pi$. This method is analogous to the design of maximally-flat, zero-phase, finite-length, low-pass filters described by Kaiser (1979). Like the basis function method described above, this "maximally-flat" method has been observed to yield a stable extrapolation filter for some choice of M . However, the phase errors obtained with the maximally-flat method exceed those obtained with the basis function method, particularly for low normalized frequencies.